

Research paper

Stochastic P-bifurcation and stochastic resonance in a noisy bistable fractional-order system



J.H. Yang^{a,b,*}, Miguel A.F. Sanjuán^c, H.G. Liu^a, G. Litak^d, X. Li^e

^aSchool of Mechatronic Engineering, China University of Mining and Technology, Xuzhou 221116, P.R. China

^bJiangsu Key Laboratory of Mine Mechanical and Electrical Equipment, China University of Mining and Technology, Xuzhou 221116, P.R. China

^cNonlinear Dynamics, Chaos and Complex Systems Group, Departamento de Física, Universidad Rey Juan Carlos, Tulipán s/n, Móstoles 28933, Madrid, Spain

^dFaculty of Mechanical Engineering, Lublin University of Technology, 36 Nadbystrzycka, Lublin 20618, Poland

^eState Key Lab of Mechanics and Control for Mechanical Structures, College of Aerospace Engineering, Nanjing University of Aeronautics and Astronautics, 29 YuDao Street, Nanjing 210016, P.R. China

ARTICLE INFO

Article history:

Received 23 December 2015

Revised 4 April 2016

Accepted 1 May 2016

Available online 4 May 2016

Keywords:

P-bifurcation

Stochastic resonance

Fractional-order calculus

ABSTRACT

We investigate the stochastic response of a noisy bistable fractional-order system when the fractional-order lies in the interval $(0, 2]$. We focus mainly on the stochastic P-bifurcation and the phenomenon of the stochastic resonance. We compare the generalized Euler algorithm and the predictor-corrector approach which are commonly used for numerical calculations of fractional-order nonlinear equations. Based on the predictor-corrector approach, the stochastic P-bifurcation and the stochastic resonance are investigated. Both the fractional-order value and the noise intensity can induce a stochastic P-bifurcation. The fractional-order may lead the stationary probability density function to turn from a single-peak mode to a double-peak mode. However, the noise intensity may transform the stationary probability density function from a double-peak mode to a single-peak mode. The stochastic resonance is investigated thoroughly, according to the linear and the nonlinear response theory. In the linear response theory, the optimal stochastic resonance may occur when the value of the fractional-order is larger than one. In previous works, the fractional-order is usually limited to the interval $(0, 1]$. Moreover, the stochastic resonance at the subharmonic frequency and the superharmonic frequency are investigated respectively, by using the nonlinear response theory. When it occurs at the subharmonic frequency, the resonance may be strong and cannot be ignored. When it occurs at the superharmonic frequency, the resonance is weak. We believe that the results in this paper might be useful for the signal processing of nonlinear systems.

© 2016 Elsevier B.V. All rights reserved.

1. Introduction

Fractional-order systems under different excitations usually show various dynamical behaviors. For example, a fractional-order system under the two-frequency excitation may present various bifurcations, such as the pitchfork bifurcation [1,2], the saddle-node bifurcation [3], the bifurcation transition from the transcritical type to the saddle-node type [4], etc. If a

* Corresponding author.

E-mail address: jianhuayang@cumt.edu.cn (J.H. Yang).

fractional-order system is excited by a random noise, stochastic resonance [5,6], stochastic coherence [7], or an stochastic jump [8–10] may occur as a response.

According to the property of the damping materials, the value of the fractional-order of a damping is usually chosen in the interval (0, 2] [11]. The system presents very different properties for the case in which the fractional-order value lies in the interval (0, 1] and the case when it lies in the interval (1, 2]. For example, in an overdamped bistable system, the vibrational resonance phenomenon at the low-frequency presents a single-resonance pattern when the fractional-order lies in the interval (0, 1]. However, it presents a double-resonance pattern when the fractional-order lies in the interval (1, 2]. In other words, the fractional-order will induce a bifurcation in the vibrational resonance pattern [1]. For multi-degree-of-freedom nonlinear oscillators with fractional-damping and excited by Gaussian white noises, for a fixed noise strength, the stochastic stability will enhance with the increase of the fractional-order when the fractional-order lies in the interval (0, 1]. However, the stochastic stability will decrease with an increase of the fractional-order when it lies in the interval (1, 2] [12]. In some of the references on fractional-order systems, the value of the fractional-order is usually limited to the interval (0, 1]. This is because the fractional-order value in (1, 2] can be changed to the interval (0, 1] through a transformation [13]. However, if we ignore the fractional-order in the interval (1, 2] and investigate the problem only in the interval (0, 1], many important results may be lost in the investigation. This is what happens with stochastic resonance, where most authors simply consider the fractional-order value in the interval (0, 1] [5,6,14]. Although some interesting results are given in these works, unfortunately we do not know much when the fractional-order value lies in the interval (1, 2]. Hence, in this work, we have decided to analyze some dynamical properties of a stochastic fractional-order system when the fractional-order value lies in the interval (0, 2].

The present paper is organized as follows. In Section 2, we compared two numerical algorithms for fractional-order nonlinear systems. In Section 3, the stochastic P-bifurcation behaviors induced by the fractional-order and the noise intensity are investigated respectively. In Section 4, the stochastic resonance at the driving frequency, the subharmonic frequency and the superharmonic frequency are studied thoroughly according to the linear and nonlinear response theory. In the last section, the main conclusions of this work are given.

2. Numerical algorithms for the fractional-order nonlinear system

There are several kinds of numerical algorithms to discretize the fractional-order nonlinear equation. For a fractional-order nonlinear equation

$$\frac{d^\alpha x}{dt^\alpha} = f(x) + N(t), \quad \alpha \in [0, 2], \tag{1}$$

herein, $f(x)$ is a nonlinear function and $N(t)$ is an excitation, either in a deterministic or random form. There are usually three definitions for the fractional-order differential operator: the Riemann-Liouville definition, the Caputo definition and the Grünwald-Letnikov definition [15,16]. The Grünwald-Letnikov is commonly used for its simplicity in numerical discretization. According to the Grünwald-Letnikov definition, the fractional-order differential operator is specifically given as follows

$$\frac{d^\alpha x(t)}{dt^\alpha} \Big|_{t=kh} = \lim_{h \rightarrow 0} \frac{1}{h^\alpha} \sum_{j=0}^k (-1)^j \binom{\alpha}{j} f(kh - jh), \tag{2}$$

with the binomial coefficient

$$\binom{\alpha}{j} = \frac{\Gamma(\alpha + 1)}{\Gamma(j + 1)\Gamma(\alpha - j + 1)}, \tag{3}$$

where $\Gamma(\cdot)$ is the Gamma function. Letting $w_j^\alpha = (-1)^j \binom{\alpha}{j}$, according to [16], we have

$$w_0^\alpha = 1, \quad w_k^\alpha = \left(1 - \frac{\alpha + 1}{k}\right) w_{k-1}^\alpha, \quad k = 1, 2, \dots, n. \tag{4}$$

If $\alpha = 1$, Eq. (4) reduces to

$$w_0^1 = 1, \quad w_1^1 = -1, \quad w_k^1 = 0, \quad k = 2, \dots, n. \tag{5}$$

For the special case $\alpha = 1$, the fractional-order operator under the Grünwald-Letnikov definition turns to the ordinary differential operator

$$\frac{dx(t)}{dt} = \lim_{h \rightarrow 0} \frac{x(t) - x(t - h)}{h}. \tag{6}$$

For numerical calculations, we should construct the white noise series at first. If $N(t)$ is a white noise with statistical properties

$$\langle N(t) \rangle = 0, \quad \langle N(t)N(s) \rangle = \sigma \delta(t - s), \tag{7}$$

according to [17], the time series of a white noise can be constructed by the following series

$$N(k) = \sqrt{\frac{\sigma}{h}} \xi(k), \quad k = 1, 2, \dots, n, \tag{8}$$

where $\xi(\bullet)$ presents the random numbers with the standard normal distribution. $\xi(\bullet)$ can be produced directly by a software such as MATLAB. Substituting Eq. (4) into Eq. (2), under the zero initial conditions, the fractional-order operator is discretized to

$$\lim_{h \rightarrow 0} \frac{1}{h^\alpha} \left[x(k) + \sum_{j=1}^{k-1} w_j^\alpha x(k-j) \right] = f[x(k-1)] + N(k-1). \tag{9}$$

For a small value of h , the limitation symbol can be deleted. Then, we obtain

$$x(k) = - \sum_{j=1}^{k-1} w_j^\alpha x(k-j) + h^\alpha \{ f[x(k-1)] + N(k-1) \}. \tag{10}$$

As a result, the fractional-order differential equation is discretized by using Eq. (10) in a generalized Euler scheme. For the special case $\alpha = 1$, Eq. (10) reduces to the algorithm in the ordinary Euler scheme,

$$x(k) = x(k-1) + h \{ f[x(k-1)] + N(k-1) \}. \tag{11}$$

If we substitute Eq. (8) into Eq. (10), we will obtain the numerical iterative algorithm for the stochastic fractional-order equation. However, if we substitute Eq. (8) into Eq. (11), we will obtain the numerical iterative algorithm for the classical Langevin equation.

When Eq. (10) is used to solve a fractional-order nonlinear equation, there are some shortcomings. At first, Eq. (10) is obtained by the zero initial conditions. However, the initial conditions are non-zero in some engineering problems. We cannot use Eq. (10) in this case. Second, the Euler algorithm is not suitable for a nonlinear equation. And the reason is because the error between the exact and the numerical solution will increase much with the iterations, so that the numerical solution would be far from the exact one with the increase of n . To avoid these technical problems, the Caputo definition can be used. The Caputo definition is given as

$$\frac{d^\alpha x}{dt^\alpha} = \frac{1}{\Gamma(m-\alpha)} \int_0^t \frac{f^{(m)}(\tau)}{(t-\tau)^{\alpha-m+1}} d\tau, \tag{12}$$

where $m-1 < \alpha < m$, $m \in N$. Besides the Euler method in Eq. (10), there are some other numerical algorithms for a fractional-order equation, such as the Newton-Leipnik-Maruyama algorithm [7,18,19], the predictor-corrector algorithm [20–22], etc. Among them, the predictor-corrector algorithm works well for numerical simulations. Under the arbitrary initial condition $x(0) = x_0$, the following iterative formula is used based on the predictor-corrector algorithm,

$$x(k+1) = x_0 + \frac{h^\alpha}{\Gamma(\alpha+2)} [f(x_p(k+1)) + N(k+1)] + \frac{h^\alpha}{\Gamma(\alpha+2)} \sum_{i=0}^k a_{i,k+1} [f(x(k)) + N(k)], \tag{13}$$

where $a_{i,k+1}$ denotes the weight of the corrector in the form

$$a_{i,k+1} = \begin{cases} k^{\alpha+1} - (k-\alpha)(k+1)^\alpha & i = 0 \\ (k-i+2)^{\alpha+1} - (k-i)^{\alpha+1} - 2(k-i+1)^{\alpha+1} & 1 \leq i \leq k \end{cases} \tag{14}$$

The expression $x_p(k+1)$ denotes the predicted value and is governed by

$$x_p(k+1) = x_0 + \frac{1}{\Gamma(\alpha)} \sum_{i=0}^k b_{i,k+1} [f(x(k)) + N(k)], \tag{15}$$

where $b_{i,k+1}$ denotes the weight of the predictor which is described as

$$b_{i,k+1} = \frac{h^\alpha}{\alpha} [(k-i+1)^\alpha - (k-i)^\alpha]. \tag{16}$$

As an example, we take $f(x) = x - x^3$ and $N(t) = R \cos(\omega t)$. The time series of Eq. (1) are given by both Euler algorithm in Eq. (10) and the predictor-corrector algorithm in Eq. (13). In Figs. 1(b)–(d), the plots drawn using the two numerical approaches are in good agreement. It verifies the validity of the numerical algorithm. However, in Fig. 1(a), the error between the two curves is large. The result calculated by the predictor-corrector algorithm is an oscillatory motion with a certain amplitude. From the change tendency of the curve in Fig. 1(a), the response obtained by the generalized Euler algorithm may increase to infinity for a long enough time, since the numerical solution would be far from the exact one for long enough times. Hence, for a fractional-order nonlinear equation, the predictor-corrector algorithm is much better than the generalized Euler algorithm, especially when the fractional-order α is in a small value case.

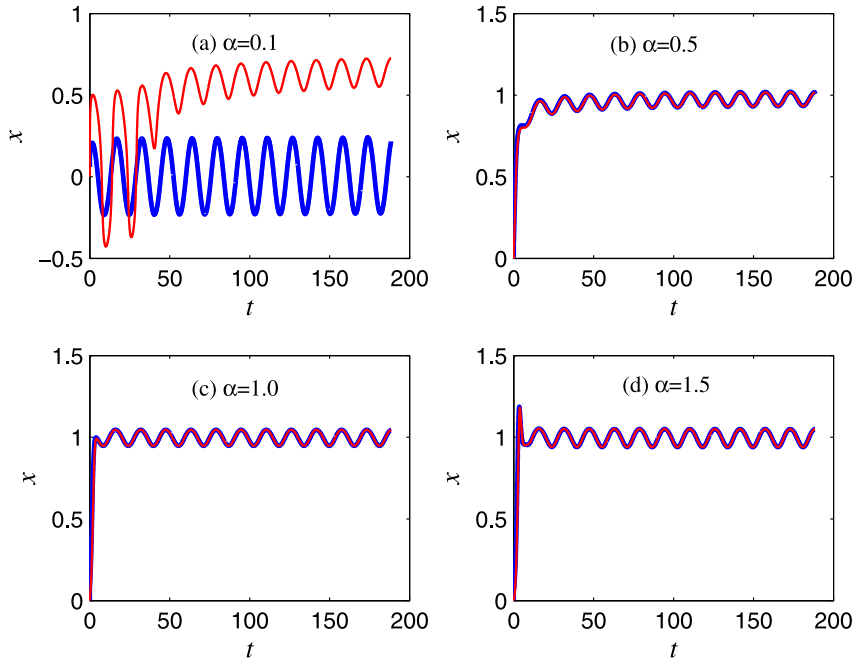


Fig. 1. The response of a fractional-order system under a periodic excitation for $R = 0.1$ and $\omega = 0.4$. The time step is $h = 0.01$ and the initial condition is $x(0) = 0$. The thin lines are obtained by the generalized Euler algorithm. The thick lines are obtained by the predictor-corrector algorithm.

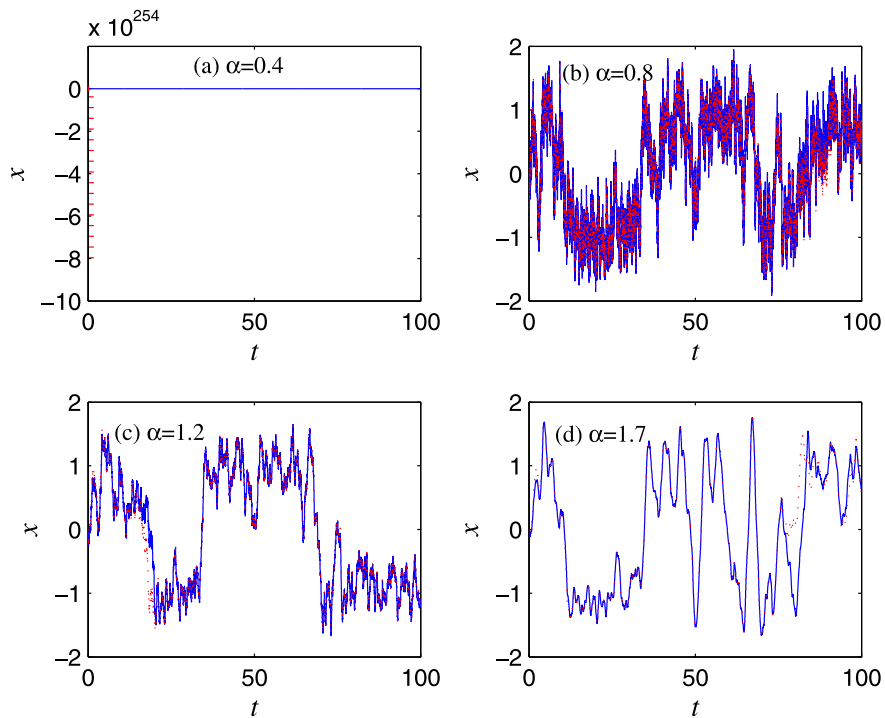


Fig. 2. The response of the fractional-order system under a white noise excitation for $\sigma = 0.4$. The time step is $h = 0.01$ and the initial condition is $x(0) = 0$. The dotted lines in the red color are obtained by the generalized Euler algorithm. The solid lines in the blue color are calculated by the predictor-corrector algorithm.

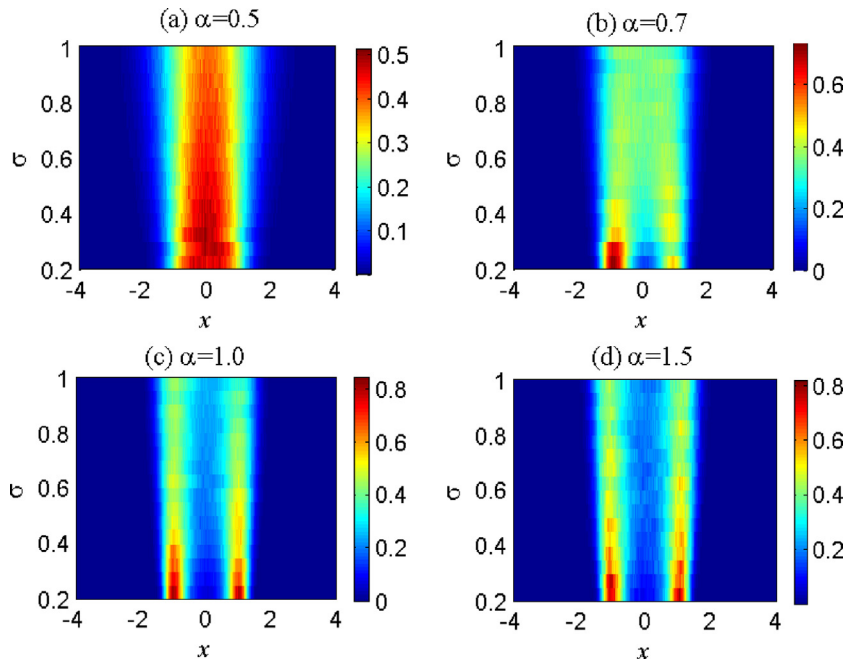


Fig. 3. Contour plot of the probability density in the $\sigma - x$ plane for different values of the fractional-order. A color code plot shows the value of the probability density.

As another example, we still take $f(x) = x - x^3$ and let $N(t)$ in a white noise form with the statistical properties in Eq. (7). If the noise intensity is $\sigma = 0.4$, the time series of Eq. (1) under the fractional-order value $\alpha = 0.4, 0.8, 1.2, 1.7$ are respectively given in Fig. 2 by the two kinds of numerical algorithms. In Fig. 2(a), for a small value of the fractional-order α , the response obtained by the generalized Euler algorithm increases to infinity rapidly. It indicates that the predictor-corrector algorithm is much better than the generalized Euler algorithm when the system is subject to random excitation.

3. The stochastic P-bifurcation

The stochastic P-bifurcation is a stochastic bifurcation phenomenon that occurs in a random system. The stochastic bifurcation contains the D-bifurcation and the P-bifurcation problems. The D-bifurcation focuses on the stochastic bifurcation point in the probability one sense which is measured by the maximal Lyapunov exponent [23]. The P-bifurcation studies the mode of the stationary probability density function or the invariant measure of the stochastic process. The stochastic P-bifurcation takes place when the mode of the stationary probability density function changes in nature. It indicates the jump of the distribution of the random variable in probability sense. The D-bifurcation and the P-bifurcation are independent. There is no direct relation between these two stochastic bifurcation phenomena [24,25].

To investigate the stochastic P-bifurcation induced by the fractional-order α and the noise intensity σ , we take a typical bistable system as $f(x) = x - x^3$ and $N(t)$ is a white noise with statistical properties shown in Eq. (7). When $\alpha = 1$, it is a classical Langevin equation and the response is a diffusion process. For this case, the response of the system can be explained as a particle moving in the potential $V(x) = \frac{x^2}{2} - \frac{x^4}{4}$ subject to random excitation. As is well known, the potential has two wells. The valley of the left well locates at $x = -1$ and the valley of the right well locates at $x = 1$. For a general fractional-order case, the random response is not a diffusion process, but a sub-diffusion process (for the case $\alpha < 1$) or a super-diffusion process (for the case $\alpha > 1$). However, in order to explain the response behavior intuitively, we still interpret the response of the fractional-order system in the sense of a particle moving in the double-well potential. The effects of the noisy intensity and the fractional-order on the probability density are illustrated in a two-dimensional plane, as shown in Fig. 3, where a color code plot of the value of the probability density appears.

If we fix the noise intensity σ as a constant and vary the fractional-order α , the probability density function is shown in Fig. 4. Apparently, with the increase of the value of the fractional-order, the mode of the stationary probability density function curve turns from a single-peak to a double-peak. It is a typical stochastic P-bifurcation behavior. Further, the stochastic P-bifurcation occurs at a critical point $\alpha < 1$. With the increase of the fractional-order α , it is harder for the particle to traverse the double-well potential. As a result, the fractional-order α is a key factor to induce the stochastic P-bifurcation phenomenon.

To verify the result in Fig. 4 much more clearly, we give Fig. 5 which shows the time series directly for different values of the fractional-order. When $\alpha = 0.5$ in Fig. 5(a), the particle traverses between the two wells frequently. When $\alpha = 0.7$ in

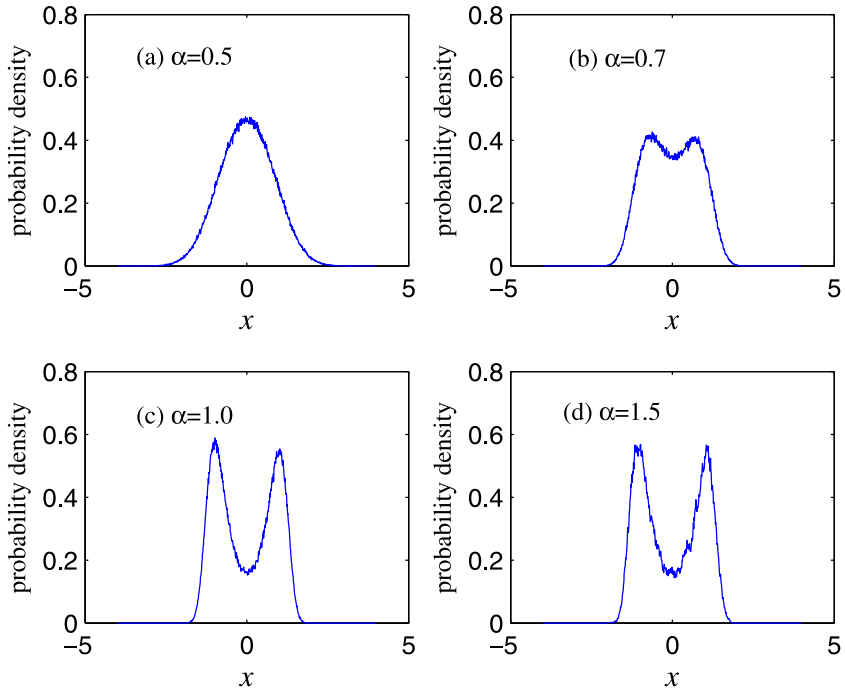


Fig. 4. The stochastic P-bifurcation is induced by the fractional-order α for a fixed noise intensity $\sigma = 0.4$.

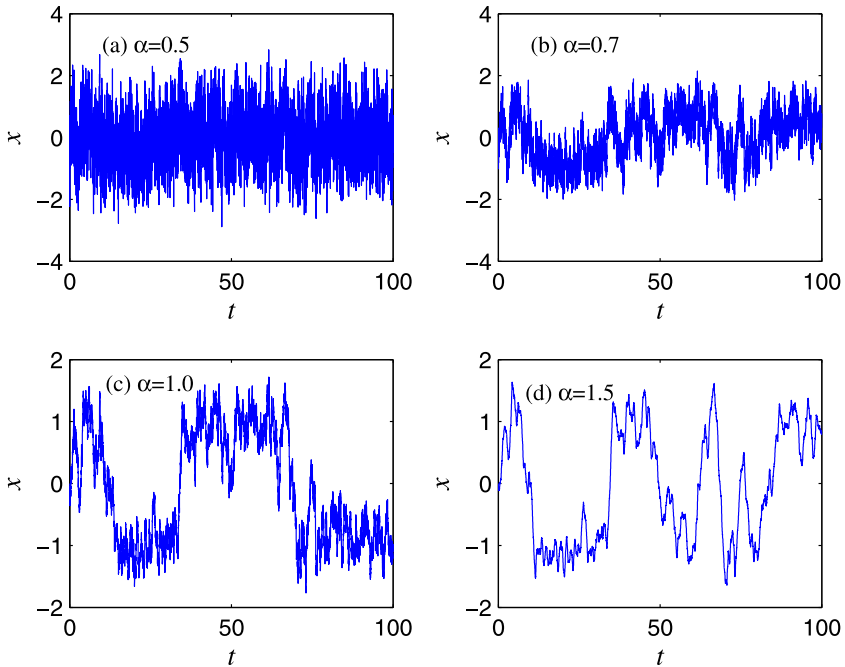


Fig. 5. The response of the fractional system subject to a Gaussian white noise excitation for $\sigma = 0.4$.

Fig. 5(b), the particle moves between the double-well potential occasionally. Apparently, for a fixed noise intensity σ , the first passage time depends on the fractional-order α closely. Hence, it is important to investigate the stochastic dynamical behaviors of the fractional system when the fractional-order value lies in the interval $(0, 2]$. We cannot ignore the case where the fractional-order value lies in the interval $(1, 2]$. Or else, we will lose many important results of a fractional-order system.

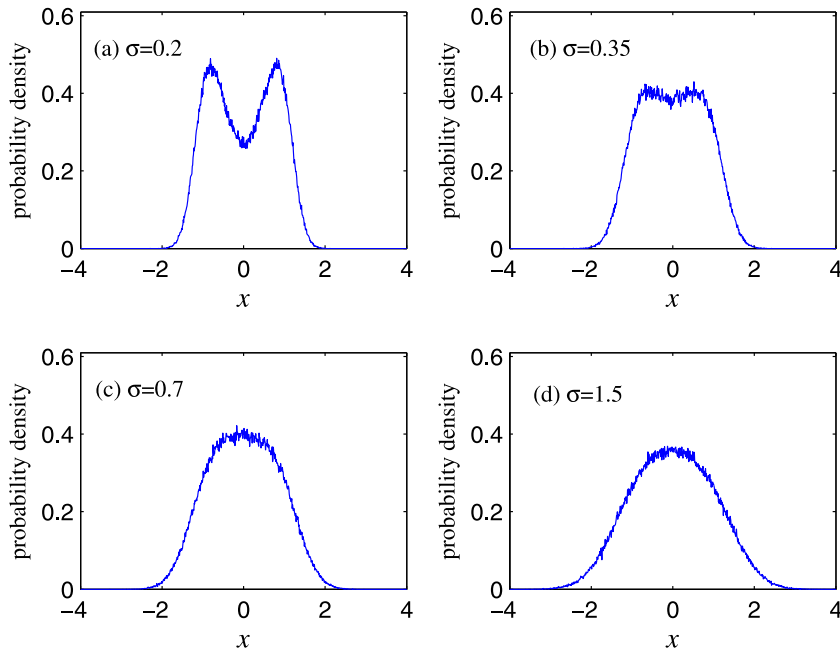


Fig. 6. The stochastic P-bifurcation is induced by various noise intensities σ for a fixed fractional-order value $\alpha = 0.65$.

In Fig. 6, we fix the fractional-order α as a constant, for example $\alpha = 0.65$, the effect of the noise intensity on the stationary probability density function is shown clearly. For the case $\sigma = 0.2$, the curve of the stationary probability density function presents a double-peak apparently, as shown in Fig. 6 (a). When we increase the noise intensity to $\sigma = 0.35$, the stationary probability density function still presents a double-peak mode. If we increase the noise intensity further, as shown in Fig. 6 (c) and Fig. 6 (d), the double-peak mode in the stationary probability density function degenerates to a single-peak. It is easy to explain this fact. Specifically, with the increase of the noise intensity, the particle is much easier to traverse the potential wells. The first passage time will turn smaller with the increase of the noise intensity for the case $\alpha = 0.65$.

As a conclusion of this section, we find that both values of the fractional-order α and the noise intensity σ are important factors to induce the stochastic P-bifurcation in a stochastic fractional-order system. The fractional-order α tends to make the stationary probability function change from a single-peak mode to a double-peak mode. The noise intensity makes a transition from the double peak mode to the single-peak mode.

4. The stochastic resonance

The stochastic resonance in the fractional-order system is not a novel topic. There are some papers on this problem [5,14,26–28] Although some interesting results are given in these works, the value of the fractional-order is usually limited to the interval $(0, 1]$ in the former works. Here, we investigate the stochastic resonance when the fractional-order lies in the interval $(0, 2]$. Note that, the stochastic resonance is usually studied in the linear response theory. In other words, we focus on the response at the excitation frequency. However, according to the nonlinear response theory, the stochastic resonance may also occur at the subharmonic/superharmonic frequencies which are smaller/larger than the excitation frequency [29–32]. Besides, the nonlinear vibration at the subharmonic or superharmonic frequencies has important consequences in the context of engineering. For example, it may indicate some fault information [33,34]. Hence, it is also necessary to study the stochastic resonance according to the nonlinear response theory.

4.1. The stochastic resonance occurs at the excitation frequency

In this section, the system for the stochastic resonance to occur is a typical bistable system which is governed by

$$\frac{d^\alpha x}{dt^\alpha} = x - x^3 + N(t) + R \cos(\omega t), \quad (17)$$

where $R \cos(\omega t)$ is the weak low-frequency signal and $N(t)$ is a Gaussian white noise with statistical properties as shown in Eq. (7). According to the nonlinear dynamical theory, the response should contain many frequency components. When the time $t \rightarrow \infty$, the asymptotic solution of Eq. (17) is in the form

$$\langle x(t) \rangle_{as} = \sum_k (k\omega) \cos[k\omega - \varphi_m(k\omega)], \quad (18)$$

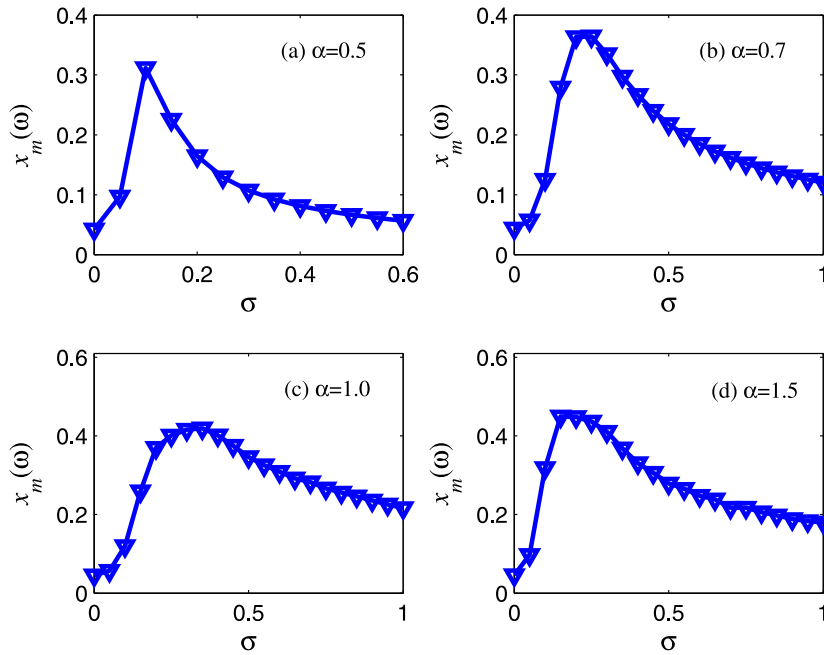


Fig. 7. The response amplitude at the excitation frequency ω versus the noise intensity σ under different fractional-order values for $R = 0.1$ and $\omega = 0.09$.

where k is a non-negative constant which may be in integer or fractional form. The expression $x_m(k\omega)$ and $\varphi_m(k\omega)$ are the mean response amplitude and the phase lag respectively at the frequency $k\omega$. They are obtained by averaging the inhomogeneous process $x(t)$ with arbitrary initial conditions $x_0 = x(t_0)$ over the ensemble of different random path realizations. For an arbitrary random path, the response amplitude at the frequency ω is \bar{x} which is calculated by

$$\bar{x} = \sqrt{B_s^2 + B_c^2}, \tag{19}$$

and

$$\bar{\varphi} = \tan^{-1}(B_s/B_c), \tag{20}$$

where B_s and B_c are the k th sine and the k th cosine components of the Fourier coefficients,

$$B_s = \frac{2}{nT} \int_0^{nT} x(t) \sin(k\omega t) dt, \quad B_c = \frac{2}{nT} \int_0^{nT} x(t) \cos(k\omega t) dt. \tag{21}$$

In Eq. (21), $T = 2\pi/\omega$ and n is a large enough integer. There are many assessment indexes to quantify the stochastic resonance phenomenon, such as the signal-to-noise ratio, the spectral amplification, etc [35]. Here, we use the response amplitude $x_m(k\omega)$ as the target for its convenient in analysis of the nonlinear response of the system.

In Fig. 7, the stochastic resonance induced by the noise intensity is shown for different values of the fractional-order α . Apparently, the value of the fractional-order influences the amount of noise and the magnitude of the response amplitude when the optimal stochastic resonance appears. Namely, in Fig. 7(a) - Fig. 7(d), the stochastic resonance occurs at $\sigma = 0.1, 0.25, 0.35, 0.15$ respectively and the corresponding magnitudes of $x_m(\omega)$ are 0.31, 0.37, 0.42, 0.45 in turn. Another important fact in this figure is that the optimal stochastic resonance in Fig. 7(d) is much stronger than that in the other three subplots. Thus, it can be seen that the optimal stochastic resonance can be achieved via the cooperation of the fractional-order α and the noise intensity σ . Hence, if we only use the classical Langevin equation to improve the stochastic resonance as our former work [36], the optimal stochastic resonance may be lost. Moreover, optimizing the stochastic resonance by adjusting the fractional-order is different from adjusting the system parameter in the former adaptive stochastic resonance investigation [37–40]. Optimizing the adaptive stochastic resonance in a fractional-order system may have preferable efficiency. Another thing, if we ignore the fractional-order in the interval $(1, 2]$ and only consider it in $(0, 1]$, we may lose the optimal stochastic resonance. This is a highlight of our results which is different from previous investigations on stochastic resonance in fractional-order systems [5,6,14,26–28].

To illustrate the stochastic resonance much more clearly, we give the time series under different noise intensity values in a fixed fractional-order case. In Fig. 8(a), the response is limited in one potential well. The particle cannot traverse the two potential wells with the excitations of the signal and the noise. There is no stochastic resonance phenomenon and the weak signal cannot be enhanced by the noise. In Fig. 8(b), the particle moves between the two wells occasionally but not regularly. The stochastic resonance has not achieved the optimal state. In Fig. 8(c), the input/output synchronization is

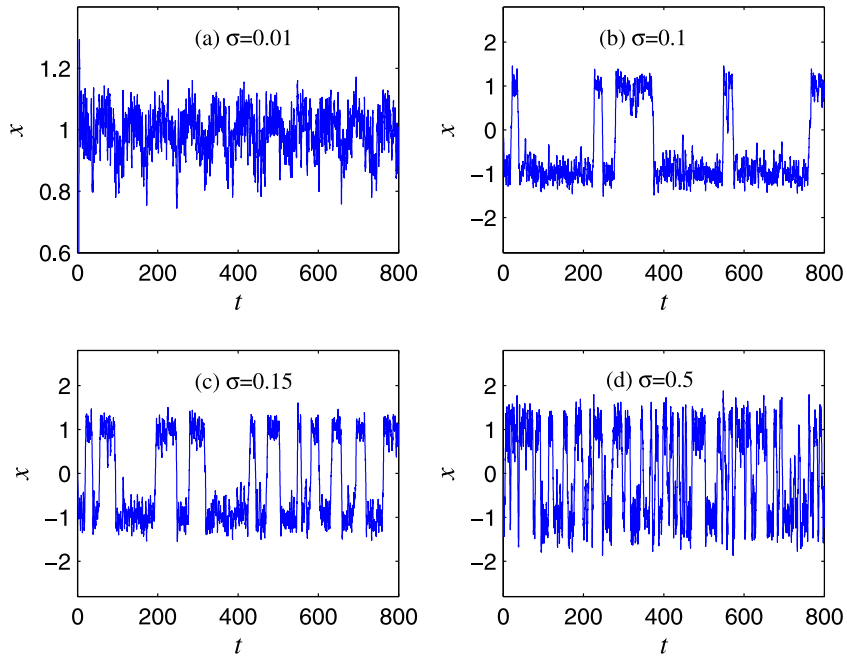


Fig. 8. The output of the fractional-order system under a fixed fractional-order and different noise intensity values for $\alpha = 1.5$, $R = 0.1$, $\omega = 0.09$.

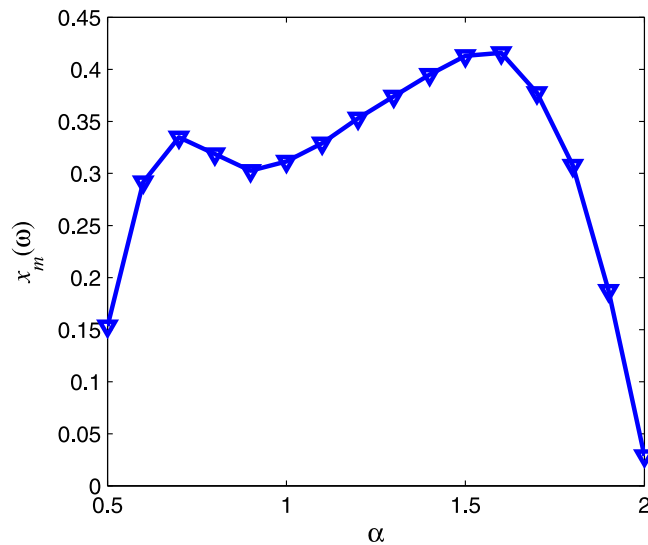


Fig. 9. The response amplitude at the excitation frequency ω versus the fractional-order α for a fixed noise intensity $\sigma = 0.2$, $R = 0.1$ and $\omega = 0.09$.

achieved. The system state changes between the two wells with the excitation period approximately. The weak signal is enhanced in a great degree. It corresponds to the resonance peak in Fig. 7(d). In Fig. 8(d), the noise intensity is too strong and the system state changes between the two wells frequently. The weak periodical signal cannot be improved in Fig. 8(d) yet. With varying the noise intensity, we can obtain the stochastic resonance in a fractional-order system. It is the same as the stochastic resonance in the classical Langevin equation.

For a fixed noise intensity, the effect of the fractional-order α on the stochastic resonance is given in Fig. 9. Apparently, the mean response amplitude at the excitation frequency ω versus the fractional-order α presents the nonlinear correlation. The value of the fractional-order α can also induce the resonance peak. Specifically, the optimal resonance occurs at the point $\alpha = 1.6$ and the peak magnitude is $x_m(\omega) = 0.42$. It indicates how important is to investigate the stochastic resonance phenomenon in the interval $\alpha \in (0, 2]$ once again.

To investigate the stochastic resonance induced by the fractional-order α thoroughly, we give Fig. 10 which can help us to understand the stochastic resonance mechanism further through the output time series. In Fig. 10(a), the particle

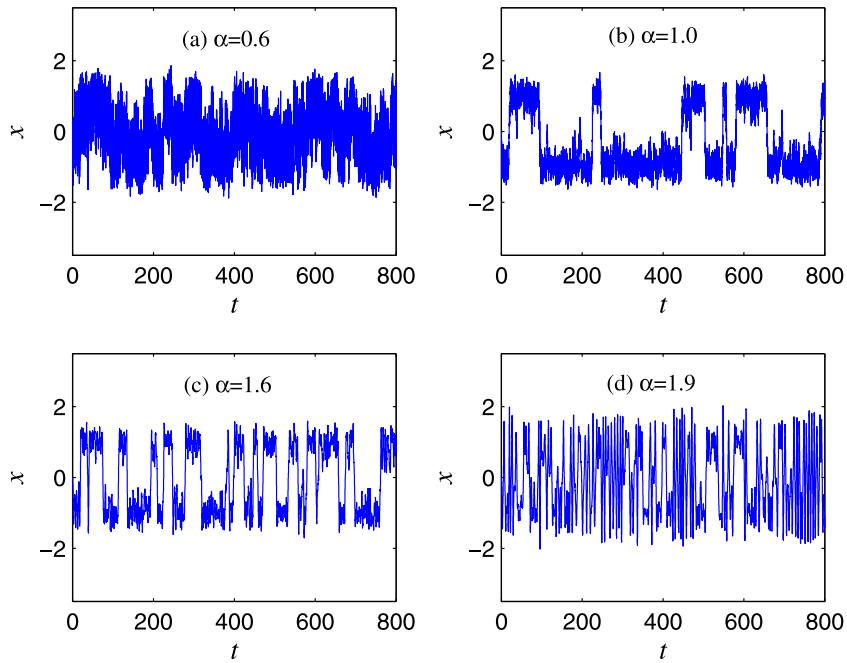


Fig. 10. The output of the fractional-order system under a fixed noise intensity and different values of the fractional-order. The simulation parameters are $\sigma = 0.5$, $R = 0.1$ and $\omega = 0.1$.

traverses the two wells frequently. There is no stochastic resonance phenomenon in this subplot. The weak signal cannot be improved in this case. It is submerged in the strong noise. In Fig. 10(b), the particle traverses the two potential wells occasionally. In Fig. 10(c), the optimal stochastic resonance is shown. It corresponds to the resonance peak in Fig. 9. From Fig. 10(a) to Fig. 10(c), the noise intensity does not change. However, the stochastic resonance appears in Fig. 10(c). It means that an appropriate fractional-order value can denoise in a great degree. It is a significant result. We still keep the noise intensity as a constant but to increase the fractional-order value to $\alpha = 1.9$, as is shown in Fig. 10(d). We find that the optimal stochastic resonance phenomenon disappears in this subplot. From Fig. 10(a) to Fig. 10(d), it indicates that we must choose an appropriate fractional-order value to obtain the optimal denoising effect. Via tuning the noise intensity to induce the stochastic resonance is different from tuning the fractional-order value to induce the stochastic resonance. Specifically, we induce the stochastic resonance via increasing the noise intensity, as is shown in Fig. 8. The energy of the noise transmits to the signal in this case. However, in Fig. 10, we induce the stochastic resonance via varying the fractional-order α which has the denoising effect in the system.

4.2. The stochastic resonance occurs at the subharmonic frequency

The stochastic resonance not only occurs at the excitation frequency ω but also occurs at the subharmonic frequency $\omega/3$. Fig. 11 shows this fact clearly. With the increase of the noise, stochastic resonance at the subharmonic frequency $\omega/3$ appears in the system. No matter the system is in the fractional order case as shown in Figs. 11(a), 11(b), 11(d) or in the integer order case as shown in Fig. 11(c). With the increase of the noise, the novel stochastic resonance occurs at the subharmonic frequency $\omega/3$ is similar to the classical stochastic resonance that occurs at the excitation frequency ω . Moreover, this kind of novel stochastic resonance is strong and we cannot ignore it in our investigation. However, there are very few works to analyze this problem in the literature. This is also another highlight of this paper. Again in Fig. 11, we find that the stochastic resonance will turn stronger with the increase of the fractional-order α . Specifically, from Fig. 11(a) to Fig. 11(d), the resonance peaks occur at $\sigma = 0.1$, 0.15, 0.15 and 0.1 in turn. The corresponding peak magnitudes are $x_m(\omega) = 0.11$, 0.24, 0.32 and 0.37. The occurrence of the stochastic resonance at the subharmonic frequency is an interesting new phenomenon.

The output of a fractional-order system under a fixed noise intensity and a fixed signal is given in Fig. 12. It corresponds to the resonance peak in Fig. 11(d). As shown in Fig. 12, it can be observed a period $3T$ where T is the period of the excitation. In other words, the frequency component $\omega/3$ is contained apparently. This is the reason for the occurrence of the novel resonance at the subharmonic frequency $\omega/3$. This extends the stochastic resonance from the traditional viewpoint. In some engineering fields, a subharmonic resonance can be a major cause for a disaster. Hence, we cannot ignore the subharmonic frequency in engineering problems.

In Fig. 13, we fixed the noise intensity σ as a constant but make the fractional-order α as the control parameter. The response amplitude is also a nonlinear function of the fractional-order. Similar to the $x_m(\omega/3) - \sigma$ curve, the stochastic

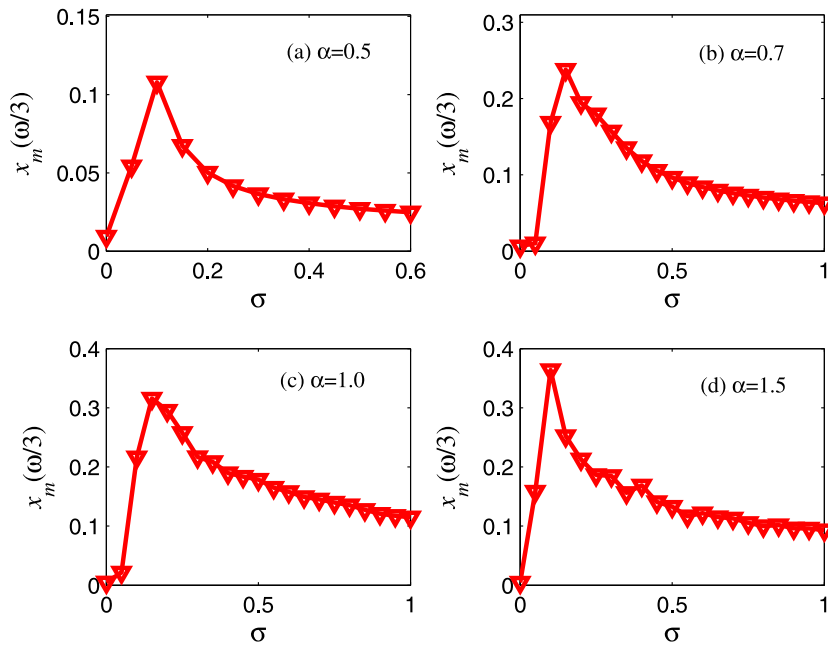


Fig. 11. The response amplitude at the subharmonic frequency $\omega/3$ versus the noise intensity σ under different fractional-order values for $R = 0.1$ and $\omega = 0.09$.

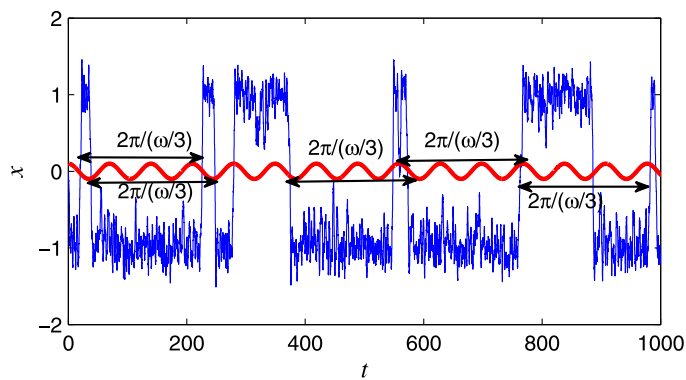


Fig. 12. The output of the fractional-order system shows the period $3T$ of the excitation. The thick line of small amplitude in red color is the input signal. The thin line in blue color is the output $x(t)$. The black lines with arrows have the same length $3T = 2\pi/(\omega/3)$. The simulation values are $\alpha = 1.5$, $\sigma = 0.1$, $R = 0.1$ and $\omega = 0.09$.

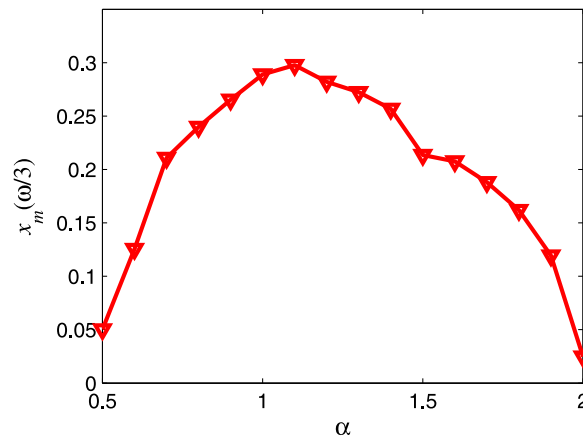


Fig. 13. The response amplitude at the subharmonic frequency $\omega/3$ versus the fractional-order for a fixed noise intensity $\sigma = 0.2$, and $R = 0.1$, $\omega = 0.09$.

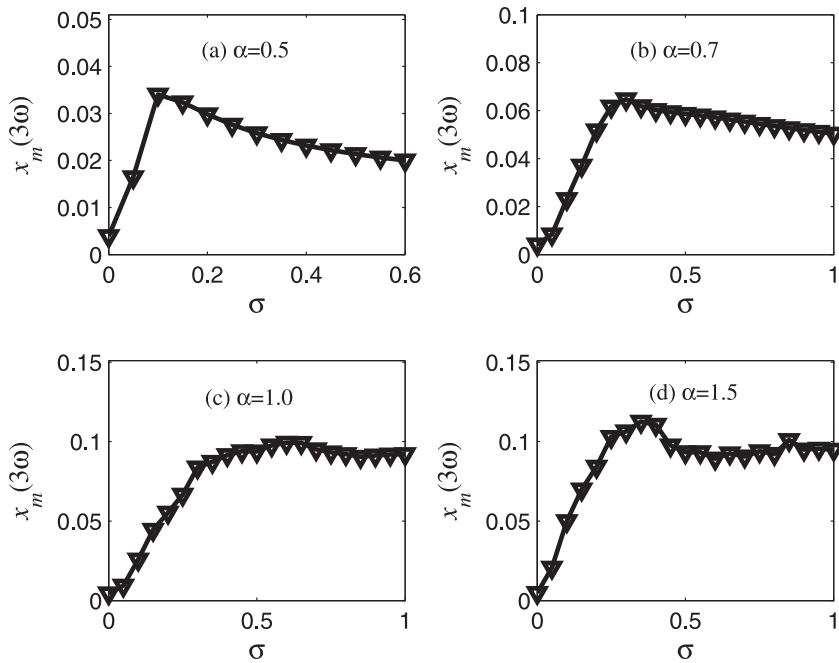


Fig. 14. The response amplitude at the superharmonic frequency 3ω versus the noise intensity σ under different fractional-order values for $R = 0.1$ and $\omega = 0.09$.

resonance at the subharmonic frequency $\omega/3$ in the $x_m(\omega/3) - \alpha$ curve appears at $\alpha = 1.1$. The corresponding peak magnitude is $x_m(\omega/3) = 0.3$. The fractional-order α is a key factor to influence the stochastic resonance at the subharmonic frequency.

4.3. The stochastic resonance occurs at the superharmonic frequency

Due to the term x^3 contained in the original system, it will lead to the component 3ω in the response. In Fig. 14, with the increase of the noise intensity, the stochastic resonance occurs at the superharmonic frequency 3ω . Compared with the traditional stochastic resonance and the subharmonic stochastic resonance, the stochastic resonance at the superharmonic frequency is weaker although the resonance phenomenon is obvious. In other words, the peak magnitude is small. This indicates that the subharmonic stochastic resonance and the traditional stochastic resonance are the main resonant patterns in the response.

In Fig. 15, for a fixed noise intensity, the fractional-order α induced superharmonic stochastic resonance is shown clearly. With the increase of α , the resonance in this curve appears at $\alpha = 1.7$ and the corresponding peak magnitude is $x_m(3\omega) = 0.12$. For the fractional-order α induced superharmonic stochastic resonance, the resonance is weak too.

5. Conclusions

In this work, we have investigated the stochastic resonance in a fractional-order bistable system excited by a Gaussian white noise. We have mainly focused on three points in this paper: the algorithm for the fractional nonlinear system, the P-bifurcation induced by the fractional-order and the noise and the corresponding induced stochastic resonance by using the linear and nonlinear response theory. In our study, the fractional-order lies in the interval $(0, 2]$.

For the first problem, two numerical algorithms are used based on the Grünwald-Letnikov definition and the Caputo definition. Corresponding to the Grünwald-Letnikov definition, the generalized Euler scheme has been used. Corresponding to the Caputo definition, the predictor-corrector approach is described in a detailed manner. We have verified the two algorithms when the excitation is deterministic and when it is random, respectively. The numerical results show that the predictor-corrector approach is much better than the generalized Euler method for the numerical calculations.

For the second problem, we have investigated the stochastic P-bifurcation in the bistable system induced by the fractional-order and the noise intensity, respectively. In a strong noise background, the stationary probability distribution function is in a single-peak mode. We fix the noise intensity but vary the fractional-order value, the stationary probability distribution function turns to a double-peak mode. The noise is suppressed in the process when the stationary probability distribution function turns from a single peak mode to a double-peak mode.

For the third problem, we have studied the stochastic resonance in the linear and nonlinear response theory, respectively. In the linear response theory, the stochastic resonance occurs at the excitation frequency for any value of the

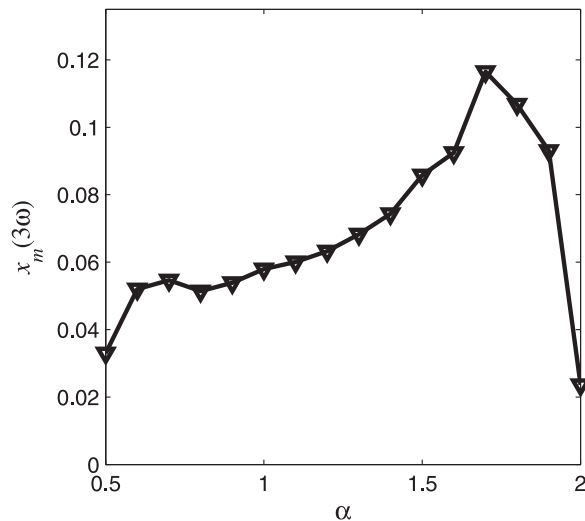


Fig. 15. The response amplitude at the superharmonic frequency 3ω versus the fractional-order for a fixed noise intensity $\sigma = 0.2$, $R = 0.1$ and $\omega = 0.09$.

fractional-order. For a fixed fractional-order, the stochastic resonance occurs by tuning the noise intensity. For a fixed noise intensity, the stochastic resonance occurs by tuning the fractional-order. Especially when the background noise is strong, the stochastic resonance appears by simply tuning the value of the fractional-order. This indicates a denoising effect of the fractional-order system. In the nonlinear response theory, the stochastic resonance appears at the subharmonic frequency or at the superharmonic frequency. We take $1/3$ and 3 times of the excitation frequency as examples. Especially when the stochastic resonance occurs at the subharmonic frequency, the response is in a strong resonant state. In the nonlinear response theory, the stochastic resonance at the subharmonic or the superharmonic frequencies can be realized by tuning the noise intensity or the fractional-order value. In many situations, the response at the subharmonic or superharmonic frequencies cannot be ignored. This is one of highlights of this work.

By investigating the stochastic P-bifurcation and the stochastic resonance in the fractional-order nonlinear system in a wide scope of the fractional-order value, some novel results are given in this work. We think our results might be useful for stochastic dynamics problems, especially for signal processing problems.

Acknowledgements

J. H. Yang acknowledges financial supports by the [National Natural Science Foundation of China](#) (Grant No 51305441), Top-notch Academic Programs Project of Jiangsu Higher Education Institutions and the Priority Academic Program Development of Jiangsu Higher Education Institutions. Miguel A. F. Sanjuán acknowledges financial support by the Spanish Ministry of Economy and Competitiveness (Grant No FIS2013-40653-P). X. Li acknowledges financial supports by the [National Natural Science Foundation of China](#) (Grant No 11472126).

References

- [1] Yang JH, Zhu H. Vibrational resonance in duffing systems with fractional-order damping. *Chaos* 2012;22:013112.
- [2] Yang JH, Zhu H. Bifurcation and resonance induced by fractional-order damping and time delay feedback in a duffing system. *Commun Nonlinear Sci Numer Simulat* 2013;18:1316–26.
- [3] Yang JH, Yang HF, Sanjuán MAF, Tian F. Saddle-node bifurcation and vibrational resonance in a fractional system with an asymmetric bistable potential. *Int J Bifurcat Chaos* 2015;25:1550023.
- [4] Yang JH, Sanjuán MAF, Liu HG, Cheng G. Bifurcation transition and nonlinear response in a fractional-order system. *J Comput Nonlin Dyn* 2015;10:061017.
- [5] He GT, Luo MK. Weak signal frequency detection based on a fractional-order bistable system. *Chin Phys Lett* 2012;29:60204.
- [6] Gao SL. Generalized stochastic resonance in a linear fractional system with a random delay. *J Stat Mech: Theory Exp* 2012;2012:P12011.
- [7] Litak G, Borowiec M. On simulation of a bistable system with fractional damping in the presence of stochastic coherence resonance. *Nonlinear Dynam* 2014;77:681–6.
- [8] Chen L, Zhu W. Stochastic jump and bifurcation of duffing oscillator with fractional derivative damping under combined harmonic and white noise excitations. *Int J NonLin Mech* 2011;46:1324–9.
- [9] Hu F, Chen LC, Zhu WQ. Stationary response of strongly non-linear oscillator with fractional derivative damping under bounded noise excitation. *Int J NonLin Mech* 2012;47:1081–7.
- [10] Xu Y, Li Y, Liu D. Response of fractional oscillators with viscoelastic term under random excitation. *J Comput Nonlin Dyn* 2014;9:1081–9.
- [11] Caponetto R, Dongola G, Fortuna L, Petráš I. *Fractional Order Systems: Modeling and Control*. Singapore: World Scientific; 2010.
- [12] Chen LC, Li HF, Li ZS, Zhu W. Stochastic stability of the harmonically and randomly excited duffing oscillator with damping modeled by a fractional derivative. *Sci China-Phys Mech Astron* 2012;55:2284–9.
- [13] Li C, Zhang F, Kurths J, Zeng F. Equivalent system for a multiple-rational-order fractional differential system. *Philos T Roy Soc A* 2013;371:20120156.
- [14] He G, Tian Y, Luo M. Stochastic resonance in an underdamped fractional oscillator with signal-modulated noise. *J Stat Mech: Theory Exp* 2014;2014:P05018.

- [15] Petráš I. Fractional-order nonlinear systems: modeling, analysis and simulation. Beijing: Higher Education Press; 2011.
- [16] Monje CA, Chen YQ, Vinagre BM, Xue D, Feliu V. Fractional-order systems and controls: fundamentals and applications. London: Springer-Verlag; 2010.
- [17] Zhu WQ. Random vibration. Beijing: Science Press; 1992. p. 371–2.
- [18] Naess A, Moe V. Efficient path integration methods for nonlinear dynamic systems. Probabilist Eng Mech 2000;15:221–31.
- [19] Litak G, Borowiec M, Wiercigroch M. Phase locking and rotational motion of a parametric pendulum in noisy and chaotic conditions. Dynam Syst 2008;23:259–65.
- [20] Deng W. Numerical algorithm for the time fractional Fokker-Planck equation. J Comput Phys 2007;227:1510–22.
- [21] Kai D, Ford NJ, Freed AD. A predictor-corrector approach for the numerical solution of fractional differential equations. Nonlinear Dynam 2002;29:3–22.
- [22] Yang Y, Xu W, Gu X, Sun Y. Stochastic response of a class of self-excited systems with Caputo-type fractional derivative driven by Gaussian white noise. Chaos Soliton Fract 2015;77:190–204.
- [23] Arnold L. Random dynamical systems. Berlin: Springer; 1998.
- [24] Yang J, Cai X, Liu X. The maximal lyapunov exponent for a three-dimensional system driven by white noise. Commun Nonlinear Sci Numer Simulat 2010;15:3498–506.
- [25] Yang JH, Hu DL, Li SH, Liu X. On stationary probability density and maximal lyapunov exponent of a co-dimension two bifurcation system subjected to parametric excitation by real noise. Int J Nonlin Mech 2011;46:186–96.
- [26] Yim MY, Liu KL. Linear response and stochastic resonance of subdiffusive bistable fractional Fokker-Planck, systems. Phys A 2006;369:329–42.
- [27] He C, Tian Y, Wang Y. Stochastic resonance in a fractional oscillator with random damping strength and random spring stiffness. J Stat Mech: Theory Exp 2013;2013:1267–79.
- [28] Goychuk I, Kharchenko V. Fractional brownian motors and stochastic resonance. Phys Rev E 2012;85:051131.
- [29] Kang YM, Xu JX, Xie Y. A method of moments for calculating dynamic responses beyond linear response theory. Chin Phys 2005;14:1691–7.
- [30] Kang YM, Jiang YL. Observing bifurcation and resonance in a mean-field coupled periodically driven noisy overdamped oscillators by the method of moments. Chaos Soliton Fract 2009;41:1987–93.
- [31] Evstigneev M, Pankov V, Prince RH. Application of the method of moments for calculating the dynamic response of periodically driven nonlinear stochastic systems. J Phys A: Math Gen 2001;34:2595–605.
- [32] Dhara AK. Signal amplification factor in stochastic resonance: an analytic non-perturbative approach. Physica D 2015;303:1–17.
- [33] Wu F, Qu L. Diagnosis of subharmonic faults of large rotating machinery based on EMD. Mech Syst Signal Pr 2009;23:467–75.
- [34] Yao H, Han Q, Li L, Wen B. Detection of rubbing location in rotor system by super-harmonic responses. J Mech Sci Technol 2012;26:2431–7.
- [35] Gammaitoni L, Hänggi P, Jung P, Marchesoni F. Stochastic resonance. Rev Mod Phys 1998;70:223–87.
- [36] Liu XL, Yang JH, Liu HG, Cheng G, Chen XH, Xu D. Optimizing the adaptive stochastic resonance and its application in fault diagnosis. Fluc Noise Lett 2015;14:1550038.
- [37] Lei Y, Han D, Lin J, He Z. Planetary gearbox fault diagnosis using an adaptive stochastic resonance method. Mech Syst Signal Pr 2013;38:113–24.
- [38] Li J, Chen X, He Z. Adaptive stochastic resonance method for impact signal detection based on sliding window. Mech Syst Signal Pr 2013;36:240–55.
- [39] Gao Y, Wang F. Adaptive cascaded-bistable stochastic resonance system research and design. J Comput Theor Nanos 2013;10:318–22.
- [40] Wu X, Jiang ZP, Repperger DW. Enhancement of stochastic resonance with tuning noise and system parameters. World congress on intelligent control and automation 2006;1:1823–7.